

MOL#77149

**Fyn inhibition by cycloalkane-fused 1,2-dithiole-3-thiones enhances
antioxidant capacity and protects mitochondria from oxidative injury**

Ja Hyun Koo, Woo Hyung Lee, Chan Gyu Lee, and Sang Geon Kim

Innovative Drug Research Center for Metabolic and Inflammatory Disease, College of Pharmacy and

Research Institute of Pharmaceutical Sciences, Seoul National University, Seoul 151-742, Korea

Running title: Mitochondrial protection by Fyn inhibition

To whom correspondence should be addressed:

Sang Geon Kim, Ph.D., College of Pharmacy, Seoul National University, Sillim-dong, Kwanak-gu,
Seoul 151-742, Korea; Tel. +822-880-7840; Fax. +822-872-1795; E-mail: sgk@snu.ac.kr

The information of manuscript statistics:

Number of Text Pages: 26

Number of Tables: 0

Number of Figures: 8

Number of References: 55

Words in Abstract: 249

Words in Introduction: 518

Words in Discussion: 1317

The abbreviations used are:

AA, arachidonic acid; ACC, acetyl-CoA carboxylase; AMPK, AMP-activated protein kinase; CDT, cycloalkane-fused dithiolethione; DCFH-DA, 2',7'-dichlorofluorescein diacetate; FACS, fluorescence-activated cell sorter; GSK3 β , glycogen synthase kinase 3 β ; LKB1, liver kinase b1; MMP, mitochondrial membrane potential; MTT, 3-(4,5-dimethylthiazol-2-yl)-2,5-diphenyl-tetrazolium bromide; Nrf2, NF-E2-related factor-2; Rh123, rhodamine 123; ROS, reactive oxygen species

ABSTRACT. Fyn kinase has emerged as a regulator of diverse pathological processes. However, therapeutic Fyn inhibitor is not available. This study investigated the potential of a series of cycloalkane-fused dithiolethiones (CDTs) or other congeners in increasing antioxidant capacity in association with Fyn inhibition and the molecular basis for this effect. Treatment of HepG2 cells with each agent protected the mitochondria from oxidative injury elicited by arachidonic acid and iron, increasing cell viability; 4,5,6,7-tetrahydrobenzo-1,2-dithiole-3-thione (SNU1A) and 5,6-dihydro-4H-cyclopenta-1,2-dithiole-3-thione (SNU2A) were the most effective, whereas 5-methyl-1,2-dithiole-3-thione (SNU3A) was less active. 5-(Quinolin-2-yl)-1,2-dithiole-3-thione (SNU3E) had a minimal effect. SNU1A treatment decreased mitochondrial superoxide production, and enabled cells to restore mitochondrial membrane permeability. Oxidative injury by arachidonic acid and iron enhanced Fyn phosphorylation at tyrosine residue, which was diminished by SNU1A treatment. SU6656, a known Fyn inhibitor, had a similar effect. Fyn inhibition contributed to protecting mitochondria from injury through AMP-activated protein kinase (AMPK), as supported by reversal of this effect by Fyn overexpression. Consistently, Fyn overexpression attenuated AMPK activation by SNU1A, strengthening the inhibitory role of Fyn in AMPK activity. CDTs had an antioxidant effect, as shown by an increase in the GSH content and the inhibition in H₂O₂ production. Moreover, they had the ability to activate Nrf2, a key antioxidant transcription factor. Fyn overexpression diminished Nrf2 activation induced by SNU1A. Our results demonstrate that CDTs have a cytoprotective effect by protecting the mitochondria and increasing cellular antioxidant capacity, and which may result from not only Fyn inhibition leading to AMPK activation, but Nrf2 activation.

INTRODUCTION

4-Methyl-5-(2-pyrazinyl)-1,2-dithiole-3-thione (oltipraz), a prototype 1,2-dithiole-3-thione, has been comprehensively investigated as a chemopreventive agent against cancer (Bolton et al., 1993; Jacobson et al., 1997; Wang et al., 1999; Kang et al., 2003). Oltipraz treatment induces phase 2 enzymes including glutathione S-transferase, UDP-glucuronyltransferase and heme oxygenase-1, which contributes to inhibiting the formation of carcinogen-DNA adducts. However, it failed to prevent oxidative DNA damage in healthy individuals (Glintborg et al., 2006). Moreover, the biotransformation of oltipraz causes variability in the pharmacokinetic profile in human (Kim et al., 2010). The efficacy and/or metabolic stability of dithiolethiones may be advanced by tailor-made design; efforts had been made to diversify candidates with the core structure of 1,2-dithiole-3-thione, some of which had the ability to diminish reactive oxygen species (ROS) in cells (Shin and Kim, 2009).

As the core of cell metabolism, mitochondria maintain the equilibrium between basal and excess levels of ROS. Under a pathological condition, the mitochondrial respiratory chain chiefly produces ROS (Browning and Horton, 2004). Since the mitochondrion functions as an energy sensor, dysfunction of the organelle determines the fate between cell survival and death (Zamzami and Kroemer, 2001). Mitochondrial permeability transition and impairment caused by oxidative stress or other stimuli promote the process of apoptosis. Conversely, preservation of mitochondrial function is important in protecting cells or organs from toxic stimuli. Therefore, it is a feasible hypothesis that agents with the ability to prevent mitochondrial dysfunction have an antioxidant and/or cytoprotective effect.

The members of Fyn/Src kinase family have emerged as the major regulators of various pathophysiological processes (Büchner et al., 2010). Several growth factors activate Fyn through the PI3K/Akt pathway (Cui et al., 2005). In skeletal muscle and adipose tissue, Fyn inhibition may contribute to regulating energy metabolism through LKB1 because Fyn phosphorylates tyrosine residues (Y261 and Y365) of LKB1 in the nucleus, preventing its cytoplasmic translocation for

inactivation (Yamada et al., 2010). Certain chemopreventive agents activate AMPK through LKB1 (Hezel and Bardeesy, 2008). Also, the agents that activate AMPK may enhance antioxidant capacity in the cell by increasing NF-E2-related factor-2 (Nrf2) activity (Liu et al., 2011). Glycogen synthase kinase 3 β (GSK3 β), a kinase inhibited by AMPK, negatively phosphorylates Nrf2, thereby repressing the antioxidative genes (Salazar et al., 2006). Hence, Fyn is likely to affect not only AMPK, but Nrf2. However, the effects of Fyn modulation by chemical means on mitochondria and antioxidant capacity remain unclear.

This study investigated whether cycloalkane-fused dithiolethiones (CDTs) or other congeners have the potential to enhance cellular antioxidant capacity in association with Fyn inhibition, and if so, what the underlying molecular basis is. In this study, we used a series of novel synthetic dithiolethione derivatives to determine their effects on antioxidant capacity and cell viability against oxidative injury elicited by arachidonic acid (AA) and iron. We were interested in identifying the effect of Fyn inhibition by the agents for the activation of AMPK, and the role of Fyn inhibition in mitochondria protection. In our findings, the ability of CDTs to impede mitochondrial permeability transition pore (mPTP) opening helps protect hepatocytes from oxidative injury. In addition, we examined the effects of CDTs on the activity of Nrf2.

MATERIALS AND METHODS

Materials. The solution of iron-nitrilotriacetic acid complex was prepared as previously described (Kim et al., 2009). MitoSOX was purchased from Molecular Probes (Carlsbad, CA). Anti-phospho-Src (pY⁴¹⁶), anti-phospho-acetyl-CoA carboxylase (ACC), anti-phospho-AMPK α , and anti-phospho-GSK3 β (pS⁹), and anti-GSK3 β antibodies were supplied from Cell Signaling Technology (Beverly, MA). Antibodies directed against AMPK were provided from Santa Cruz Biotechnology (Santa Cruz, CA). Horseradish peroxidase-conjugated goat anti-rabbit and goat anti-mouse IgGs were purchased from Zymed Laboratories (San Francisco, CA). Anti-Fyn antibody and GSH assay kit were obtained from Oxis International (Portland, OR). AA was purchased from Calbiochem (San Diego, CA). Rhodamine 123 (Rh123), 2',7'-dichlorofluorescein diacetate (DCFH-DA), 3-(4,5-dimethylthiazol-2-yl)-2,5-diphenyl-tetrazolium bromide (MTT), Compound C, anti- β -actin antibody, and other reagents were supplied from Sigma (St. Louis, MO).

Chemical synthesis. Oltipraz and its cycloalkane derivatives (Fig. 1) were provided by the CJ Central Laboratories (Ichon, Korea).

Cell culture and treatment. HepG2 cells, a human hepatocyte-derived cell line, were purchased from ATCC (Rockville, MD) and cultured in Dulbecco's modified Eagle's medium (DMEM) containing 10% fetal bovine serum (FBS), penicillin (50 units/ml), and streptomycin (50 μ g/ml) at 37°C in humidified atmosphere (5% CO₂). All experiments were performed using cells with passage number less than 15. For all experiments, the cells (1×10^6) were seeded in a 10-cm² plastic dish for 2–3 days (i.e. 80% confluency) and serum-starved for 24 h. They were treated with 10 μ M AA for 12 h, washed with minimum essential medium (MEM), and then continuously incubated with AA plus iron-nitriloacetic acid complex (iron, 5 μ M) for the indicated time period. They were treated with 1–10 μ M of each agent of interest for 1 h, followed by continuous incubation with AA and iron.

Cell cycle analysis. Cell cycle was measured using propidium iodide, as previously described (Shin and Kim, 2009). The fluorescence intensity of cells stained with propidium iodide was monitored using a BD FACS Calibur flow cytometer (San Jose, CA).

MTT assay. MTT assay was performed according to previously published methods (Shin and Kim, 2009). Absorbance was detected at 540 nm using an enzyme-linked immunosorbent assay (ELISA) microplate reader (Tecan, Research Triangle Park, NC). Cell viability was calculated relative to untreated control [i.e. viability (% control) = $100 \times (\text{absorbance of treated sample})/(\text{absorbance of control})$] (Kim et al., 2009).

Immunoblot analysis. Cell lysates were prepared according to previously published methods (Shin and Kim, 2009). Briefly, cells were centrifuged at 3,000g for 3 min and were subjected to expand osmotically to the point of lysis after the addition of lysis buffer containing 10 mM Tris-HCl (pH 7.1), 100 mM NaCl, 1 mM EDTA, 10% glycerol, 0.5% Triton X-100, 0.5% Nonidet P-40, 1 mM dithiothreitol, and 0.5 mM phenylmethylsulfonyl fluoride, as supplemented with a protease inhibitor cocktail (Calbiochem, La Jolla, CA). The lysates were centrifuged at 10,000g for 10 min to obtain supernatants and were stored at -70°C until use. Immunoblot analysis was performed according to previously published procedures (Shin and Kim, 2009). Protein bands of interest were developed using an ECL chemiluminescence system (Amersham, Buckinghamshire, UK). Equal loading of proteins was verified by immunoblotting for β -actin. Scanning densitometry was performed with an Image Scan & Analysis System (Alpha-Innotech Corporation, San Leandro, CA).

Flow cytometric analysis of mitochondrial membrane potential (MMP). MMP was measured using Rh123 as previously published (Shin and Kim, 2009). The cells in M1 fraction was measured using a BD FACS Calibur flow cytometer (San Jose, CA).

Measurement of H₂O₂ production. DCFH-DA, a cell-permeable non-fluorescent probe, is turned into the fluorescent dichlorofluorescein (DCF) upon reaction with H₂O₂ by intracellular esterases, as described previously (Shin and Kim, 2009). The level of H₂O₂ generation was determined by the concomitant increase in DCF fluorescence, which was measured using FACS (San Jose, CA).

Measurement of mitochondrial ROS. Mitochondrial ROS was monitored in HepG2 cells loaded with 5 μ M MitoSOX, a mitochondrial superoxide indicator, for 10 min, as previously published (Choi et al., 2010). The fluorescence intensity in the cells was detected using FACS (San Jose, CA).

Determination of reduced GSH content. Reduced GSH in the cell was quantified using a commercial GSH determination kit (GSH-400, Oxis International, Portland, OR), as previously described (Kay et al., 2011).

Recombinant adenoviral DN-AMPK construct. The plasmid encoding dominant-negative AMPK (DN-AMPK), which was provided by Dr. J. Ha (Kyung Hee University, Korea), was used for the preparation of its adenoviral construct. HepG2 cells were infected with adenoviral DN-AMPK diluted in DMEM containing 10% FBS at a multiplicity of infection of 50 and incubated for 12 h. After removal of the viral suspension, they were incubated with DMEM containing 10% FBS for 2 days, and were treated with the indicated agent, as described previously (Choi et al., 2010). Adenovirus that expresses LacZ (Ad-LacZ) was used as an infection control.

Transient transfection and luciferase reporter assay. Cells were plated at a density of 1×10^6 cells per well in 6-well dishes and transfected the following day according to previously published method (Kay et al., 2011). Briefly, the cells were incubated with 1 μ g of NQO1-ARE reporter plasmid and 3 μ L of FuGENE[®] HD Reagent (Roche, Indianapolis, IN) in 1 ml of antibiotic-free MEM

medium for 3 h. The ARE-luciferase reporter was provided from N. Wakabayashi (Johns Hopkins University, MD). They were incubated in a serum-free medium for 6 h, and exposed to medium containing FBS with or without the agent of interest. Luciferase activities were measured using a dual luciferase assay system (Promega, Madison, WI).

Preparation of nuclear extracts. Nuclear extracts was prepared according to a previously published method, as described previously in detail (Kay et al., 2011). The nuclear fractions were stored at -70°C until use.

Immunoprecipitation assays. To measure Fyn phosphorylation, cell lysates were incubated with anti-Fyn antibody overnight at 4°C . The antigen-antibody complex was immunoprecipitated after incubation with protein G-agarose for 2 h. Immune complexes were dissolved in $2\times$ Laemmli buffer. Protein samples were resolved and immunoblotted with anti-Src(pY⁴¹⁶) antibody.

Plasmid transfection. The plasmids encoding for wild type and a dominant negative mutant form of Fyn were obtained from Addgene (Cambridge, MA). Cells were transfected with the plasmids (1 μg) using FuGENE HD (Roche, Indianapolis, IN). The empty plasmid, pcDNA3.1 was used for the mock transfection.

In vitro kinase assay. After pre-incubation of recombinant human Fyn (Millipore, Billerica, MA) in Tris-HCl buffer (50 mM, pH 7.5) containing KVEKIGEGTYGVVYK (250 μM Cdc2 peptide), 0.1 mM EGTA, 0.1 mM Na_3VO_4 and 10 mM Mg^{++} acetate, the reaction was initiated by the addition of the mixture comprising 70 μM Mg^{++}ATP and [γ -³²P-ATP] (specific activity approx. 500 cpm/pmol) at room temperature. After incubation for 40 min, the reaction was stopped by the addition of 3% phosphoric acid solution. An aliquot of the reaction mixture (10 μL) was spotted onto a P30 filtermat, which was washed with 75 mM phosphoric acid for 5 min three times and once with methanol prior to

drying and scintillation counting.

Data analysis. One-way analysis of variance tests were used to assess the significance of differences among treatment groups. For each statistically significant effect of treatment, the Newman-Keuls test was used for comparisons between multiple group means. The data were expressed as mean \pm Standard error of the mean (S.E.M.) The criterion for statistical significance was set at $p < 0.05$ or $p < 0.01$.

RESULTS

Increases in cell survival against oxidative injury

Among the newly synthesized dithiolethiones, eleven CDTs and other 1,2-dithiole-3-thiones were selected to compare their activities on cell survival *in vitro* (Fig. 1A): we determined their effects on the viability of HepG2 cells against oxidative injury elicited by AA and iron using MTT assays. The ED₅₀ values for cell survival were in the range of 0.5-10 μ M (Fig. 1B). Among those representing each basic core structure, 4,5,6,7-tetrahydrobenzo-1,2-dithiole-3-thione (SNU1A) and 5,6-dihydro-4H-cyclopenta-1,2-dithiole-3-thione (SNU2A) were the most effective, whereas others showed lesser or minimal effect (Fig. 1B). A bulky substitution at the 5-position of 1,2-dithiole-3-thione resulted in a complete loss of activity. In subsequent experiments, we compared the effects of SNU1A, SNU2A, 5-methyl-1,2-dithiole-3-thione (SNU3A) and 5-(quinolin-2-yl)-1,2-dithiole-3-thione (SNU3E). SNU3E was used as the least active control (Fig. 2A).

The dose-response effects were depicted in Fig. 2A. SNU1A, SNU2A, SNU3A, and SNU3E had no cytotoxicity (Fig. 2A, inset). Morphological examination by light microscopy confirmed that SNU1A treatment caused an obvious protective effect against injury (Fig. 2B). Again, the agent alone showed no toxicity. To confirm an increase in cell viability by the agents, apoptotic marker proteins were measured in the lysates. AA + iron decreased the level of poly(ADP-ribose)polymerase (PARP) but increased that of cleaved caspase-3, which indicates apoptosis (Fig. 2C). Treatment with SNU1A, SNU2A or SNU3A protected cells from apoptosis (Fig. 2C). SNU3E had no effect. Our results showed that CDTs including SNU1A, SNU2A, and SNU3A have the ability to rescue the cells from oxidative stress elicited by AA and iron.

Mitochondrial protective effects

AA treatment causes dysfunction of MMP via impairment of mitochondrial respiratory activity (i.e., complexes I and III binding) (Cocco et al., 1999). Excess iron accumulation and the resultant ROS production impair mitochondrial function (George et al., 1998; Kumar and Bandyopadhyay,

2005). Next, MMP was measured using FACS analysis after staining of HepG2 cells with Rh123 (a probe of MMP). Treatment of the cells with AA + iron decreased the proportion of Rh123-positive cells, and caused an increase in the M1 fraction (i.e., the fraction with low Rh123 fluorescence intensity) (Fig. 3A). SNU1A, SNU2A or SNU3A effectively abolished the mitochondrial dysfunction, whereas SNU3E failed to do so. Since mitochondrial dysfunction disturbs oxidative phosphorylation and depletes ATP with ROS generation (Shin and Kim, 2009), we assessed whether treatment with the agents inhibits mitochondrial superoxide production using MitoSOX, a mitochondrial superoxide indicator. MitoSOX fluorescence in the mitochondria was remarkably elevated by AA + iron treatment, which was inhibited completely by SNU1A, and partially by SNU3A (Fig. 3B). Thus, both SNU1A and SNU2A most effectively protected the mitochondria from oxidative injury, and inhibited superoxide overproduction. In addition, AA + iron treatment arrested cell-cycle progression in the sub-G1 phase, which was relieved by SNU1A, but not by SNU3E (Fig. 3C). Each of these agents alone did not change the cell cycle progression (data not shown).

AMPK-dependent mitochondrial protection

AMPK plays a role in sensing intracellular energy status and is activated by various stresses such as an augmented AMP/ATP ratio. In HepG2 cells, each agent showed the ability to activate AMPK, as evidenced by an increase in the phosphorylation of AMPK or its downstream enzyme ACC (Fig. 4A). Among them, SNU1A was the most efficacious. GSK3 β , a Ser/Thr kinase constitutively active in the normal state, regulates cell viability against oxidative injury by promoting mPTP opening (Kockeritz et al., 2006). It was reported that resveratrol inhibits GSK3 β through phosphorylation as a downstream substrate of AMPK (Shin et al., 2009). Next, we examined the effects of CDTs on the serine phosphorylation of GSK3 β . As expected, treatment with each agent increased the phosphorylation of GSK3 β (Fig. 4B); SNU1A was the most effective. Ad-DN-AMPK infection diminished the ability of SNU1A to inhibit MMP transition (Fig. 4C). In addition, it decreased the basal phosphorylation of ACC or GSK3 β as well as their SNU1A-inducible phosphorylation (Fig. 4D).

All of these results demonstrate that CDTs have the ability to activate AMPK, which may be responsible for the inhibition of GSK3 β for mitochondrial protection.

Role of Fyn inhibition in the mitochondrial protection

In an effort to find the underlying basis for the antioxidant effect, we determined whether CDTs affect the activity of Fyn by monitoring its tyrosine phosphorylation. One active phosphorylation site of Fyn at tyrosine residue (Y⁴²⁰) has been identified (Pariser et al., 2005). Exposure of HepG2 cells to AA + iron caused an increase in the phosphorylation of Fyn, which was attenuated by SNU1A, SNU2A or SNU3A (Fig. 5A). SNU3E showed a weaker effect. SU6656, a known Fyn inhibitor, also inhibited the phosphorylation of Fyn. Moreover, SNU1A inhibited the basal activity of Fyn, as did SU6656 (Fig. 5B). Next, we assessed whether the CDTs had a direct inhibitory effect on Fyn using *in vitro* kinase assay; unlike SU6656, they failed to directly inhibit Fyn (Fig. 5C), suggesting that there may exist an upstream regulator of Fyn affected by the agents. To test the role of Fyn inhibition by SNU1A in protecting mitochondria from oxidative injury, the effect of Fyn overexpression on the MMP change was measured after Rh123 staining. Fyn overexpression reversed the protective effect of SNU1A against the mitochondrial injury (Fig. 5D). The CDTs had the ability to inhibit Fyn phosphorylation, which might be associated with their mitochondrial protective effect. To understand more in depth the mechanism underlying the antioxidant effect, we determined whether they activated AMPK through Fyn inhibition. Enforced expression of Fyn diminished the phosphorylation of AMPK α or ACC increased by SNU1A (Fig. 5E), suggesting that Fyn inhibition by the agent contributes to activating AMPK.

Enhancement of antioxidant capacity

Next, we analyzed the content of reduced GSH in HepG2 cells treated with AA + iron in combination with the agents. The level of GSH was significantly decreased by AA + iron treatment, which was prevented by simultaneous treatment with SNU1A, SNU2A or SNU3A (Fig. 6A, left). As

expected, SNU3E had no effect. We also found that each CDT treatment alone increased GSH levels (Fig. 6A, right). To confirm their antioxidant effect, the extent of intracellular H₂O₂ production was measured by flow cytometric assay using DCFH-DA, a specific marker for H₂O₂. Treatment with SNU1A, SNU2A and SNU3A (30 μM each) abrogated an increase in H₂O₂ production caused by AA + iron (Fig. 6B). SNU3E had no effect. Our findings also indicated that combination of Fyn overexpression and Compound C (an AMPK inhibitor) treatment significantly diminished the increase in GSH content by SNU1A (Fig. 6C), confirming the regulatory effect of the kinases on the antioxidant effect.

Nrf2-antioxidant response element activation

As a continuing effort to find the molecular basis for the cytoprotective effect, we examined the level of Nrf2, a critical transcription factor responsible for antioxidant genes expression. Pro-oxidants or low levels of ROS may activate Nrf2 (Nguyen et al., 2004). Among the agents examined, only SNU2A showed a slight increase in ROS production when treated alone, indicating that it has a pro-oxidant effect (Fig. 7A). Consistently, SNU2A increased the level of Nrf2 most effectively, as shown by increases in Nrf2 band intensity and ARE-driven reporter activity (Fig. 7B and C). SNU1A and SNU3A showed no pro-oxidant effect, but increased Nrf2 levels. SNU3E had no effect. Ad-DN-AMPK infection prevented the increases in Nrf2 level or NQO1-ARE gene transactivation by SNU1A (Fig. 7D), which supports the role of AMPK in Nrf2 activation. As an effort to link Fyn and Nrf2, we monitored the effect of Fyn overexpression on the increase in Nrf2 level by SNU1A; Fyn overexpression prevented both the accumulation of Nrf2 and the induction of ARE reporter gene (Fig. 7E). These results provide evidence that the ability of SNU1A to increase Nrf2 activity may result at least in part from Fyn inhibition leading to AMPK activation.

DISCUSSION

Oxidative stress induces mitochondrial permeability transition and alters the integrity of membrane phospholipids including AA. The oxidation of fatty acids and phospholipids activates phospholipase. AA as a ω -6 pro-inflammatory fatty acid originated from cell membranes stimulates ROS production, augmenting lipid peroxidation. In fact, an enhancement in the ratio of ω -6/ ω -3 fatty acids was detected in patients with cancer, cardiovascular disease or hepatitis (Araya et al., 2004; Dwyer et al., 2004; Simopoulos, 2006). Oxidative stress elicited by AA may have a detrimental effect on mitochondria (Cocco et al., 1999; Scorrano et al., 2001). It also increases the level of proapoptotic ceramides and calcium uptake into mitochondria. Iron causes organ damage and dysfunction. In particular, liver is susceptible to excess iron because it is the main organ for storage (McLaren et al., 1995). In an early pathological process, excess iron accumulation in non-parenchymal cells and its redistribution toward surrounding cells enhance oxidative stress. So, the presence of iron synergizes the deleterious effect of AA, provoking apoptosis. In the present study, a series of CDTs and other congeners had the ability to enhance antioxidant capacity and rescue mitochondria from oxidative injury elicited by AA plus iron. In our findings, the CDTs exhibited greater potencies in protecting cells from the oxidative injury than other dithiolethiones, suggesting that they may have beneficial effects on oxidative and inflammatory diseases.

The compounds with core dithiolethione structure have chemopreventive properties, as shown by the results of animal and clinical studies (Zhang and Munday, 2008; Kensler and Wakabayashi, 2010). Efforts have been made to develop dithiolethione derivatives with better efficacy; aryl dithiolethione compounds exert an anticancer effect through histone deacetylation (Tazzari et al., 2010), whereas anethole dithiolethiones may have a chemopreventive effect by inhibiting aryl hydrocarbon receptor pathway (Bass et al., 2009). Dithiolethiones fused with non-steroidal anti-inflammatory drugs (NSAIDs) had also been studied as anti-angiogenic agents (Isenberg et al., 2007). Oltipraz, a prototype dithiolethione, is oxidized by two major pathways common to various mammals: (1) oxidative desulfuration of the thione to yield M1 metabolite; and (2) desulfuration, methylation, and

molecular rearrangement to yield M2 metabolite (Bieder et al., 1983; O'Dwyer et al., 1997). Since biotransformation of dithiolethiones causes variability in the pharmacokinetic profiles in human (O'Dwyer et al., 2000), their efficacy and/or metabolic stability may be advanced by designing different ring structures. Cyclized compounds generally show less vulnerability against metabolic assault (Thomson, 2001). So, the CDTs may have an advantage to bypass biotransformation of ring rearrangement.

AMPK regulates energy metabolism and increases cell viability in response to pathological stresses such as endoplasmic reticulum stress, oxidative stress, and osmotic stress (Hayashi et al., 2000; Ido et al., 2002; Terai et al., 2005; Bae et al., 2008; Shin et al., 2009). Oxidative stress increases the activity of GSK3 β , and facilitates its mitochondrial translocation; activated GSK3 β phosphorylates, binds to the elements of mitochondrial membrane pore (e.g. VDAC and ANT), inducing MMP transition (Nishihara et al., 2007; Das et al., 2008). AMPK contributed to protecting mitochondria by inhibiting GSK3 β activity (Shin et al., 2009). Oltipraz has the capability to prevent mitochondrial impairment from oxidative stress by activating AMPK (Shin and Kim, 2009). Other agents such as resveratrol and isoliquiritigenin also inhibited superoxide production in mitochondria and protected them through GSK3 β phosphorylation downstream of AMPK (Shin et al., 2009; Choi et al., 2010). Our present finding that CDTs inhibited GSK3 β via AMPK activation corroborated the inhibitory effect of AMPK on GSK3 β for the protection of mitochondria.

Fyn, a member of the Src kinase family, is a constitutively expressed membrane-localized non-receptor tyrosine kinase. In the present study, the new dithiolethiones protected mitochondria by activating AMPK. Our result also shows that Fyn is an upstream molecule that controls AMPK activity, being consistent with the observation that chemical inhibition of Fyn led to AMPK activation (Bastie et al., 2007). Under the conditions of oxidative stress or osmotic shock, Fyn stimulates MAPK pathways (Abe and Berk, 1999). In our work, the negative regulation of AMPK by Fyn was inhibited by the CDTs having antioxidant activity. This is in line with the observation that Fyn knockout altered ROS-induced signaling pathways (Abe and Berk, 1999). Our finding that Fyn overexpression and

Compound C (an AMPK inhibitor) treatment significantly diminished the increase in GSH content by SNU1A supports the role of Fyn inhibition and AMPK activation in its antioxidant activity. Nevertheless, either Fyn overexpression or AMPK inhibition alone failed to significantly reverse the effect of SNU1A, suggesting that AMPK may affect Fyn activity as a feedback loop.

There are some known regulators of Fyn kinase; Fyn phosphorylation at Y⁴²⁰ residue (a major active phosphorylation) depends on autophosphorylation. Phosphorylation at Y⁵³¹ residue by CSK inhibits Fyn, whereas dephosphorylation on the same site by PTPRC/CD45 activates the overall activity (Peters et al., 1990; Mustelin et al., 1992). Since Fyn activity is associated with membrane receptor signaling (Parsons and parsons, 2004; Sandilands et al., 2007; Lu et al., 2009), SNU compounds may also modulate the upstream receptor signals (e.g., receptor tyrosine kinase). These possibilities remain to be clarified.

Despite the known effect of Fyn on cell growth and survival, little information had been available regarding its effect on mitochondria. An important finding of our study is identification of Fyn activation along with mitochondrial dysfunction; activated Fyn seems to cause impairment of mitochondrial function, and facilitate apoptosis. In the present study, the ability of new dithiolethiones to decrease Fyn phosphorylation contributed to protecting cells from oxidative stress, as supported by the finding that Fyn overexpression diminished the mitochondrial protective effect. Our results match the finding that a deficiency in Fyn decreased caspase activation and DNA fragmentation by proapoptotic stimuli in embryonic fibroblasts or thymocytes (Ricci et al., 2001; Donlin et al., 2002). The observation that SU6656 (a Fyn inhibitor) inhibits GSK3 β through phosphorylation (data not shown) also supports the hypothesis.

In the current study, CDTs (i.e., SNU1A and SNU2A) inhibited H₂O₂ production. Moreover, treatment with each of the agents enabled cells to restore GSH content. Many of AMPK activators may also enhance Nrf2 activity (Kay et al., 2010, 2011). Similarly, AMPK activation increases Nrf2 expression level (Liu et al., 2011). The possibility that Nrf2 protects mitochondria from oxidative stress irrespective of AMPK is strengthened by our observation that metformin, an AMPK activator

that lacks Nrf2-activating effect, failed to alleviate oxidative injury by AA + iron (Shin and Kim, unpublished data). Overall, it is highly likely that the antioxidant capacity of CDTs goes in parallel with the ability to activate Nrf2. In the present study, the degree of Nrf2 activation by SNU2A was greater than that by others, which may be associated with its effect on mitochondrial superoxide production (Fig. 8).

Protein kinase C, Akt and PKR-like endoplasmic reticulum kinase activate Nrf2 through phosphorylation (Nguyen et al., 2004). On the contrary, Nrf2 phosphorylation by GSK3 β diminishes its activity (Salazar et al., 2006). Our results support the notion that Nrf2 activation caused by CDTs may be linked to GSK3 β inhibition, as suggested by the finding that DN-AMPK overexpression diminished the ability of SNU1A to enhance Nrf2 activity. However, the degree of Nrf2 activation by SNU2A was much greater than other agents despite their comparable inhibitory effects on Fyn. Also, SNU2A has a pro-oxidant effect, which may account for its greater activation of Nrf2 since pro-oxidants and low levels of ROS activate Nrf2 via Keap1 oxidation (Nguyen et al., 2004). This may also account for the discrepancy between its AMPK activation and cell survival effect.

Collectively, we found CDTs as cytoprotective agents against oxidative stress, and their beneficial effect may result from improvement of mitochondrial function through Fyn inhibition, which leads to AMPK activation, and GSK3 β inhibition, consequently to Nrf2 activation (Fig. 8). Moreover, some of the agents have an additional stimulating effect on Nrf2 which further increases antioxidant capacity. Since the new dithiolethiones have the capability to protect cells from oxidative injury, they may be utilized as preventive and/or therapeutic candidates for chronic inflammatory illnesses.

AUTHORSHIP CONTRIBUTION

Participated in research design: Koo, W.H. Lee, and Kim.

Conducted experiments: Koo and C.G. Lee.

Contributed new reagents or analytic tools: Koo, W.H. Lee, and Kim.

Performed data analysis: Koo and Kim.

Wrote or contributed to the writing of the manuscript: Koo, W.H. Lee, and Kim.

REFERENCES

- Abe J and Berk BC (1999) Fyn and JAK2 mediate Ras activation by reactive oxygen species. *J Biol Chem* **274**:21003–21010.
- Araya J, Rodrigo R, Videla LA, Thielemann L, Orellana M, Pettinelli P, and Poniachik J (2004) Increase in long-chain polyunsaturated fatty acid n-6/n-3 ratio in relation to hepatic steatosis in patients with non-alcoholic fatty liver disease. *Clin Sci (Lond)* **106**:635–643.
- Bae EJ, Yang YM, and Kim SG (2008) Abrogation of hyperosmotic impairment of insulin signaling by a novel class of 1,2-dithiole-3-thiones through the inhibition of S6K1 activation. *Mol Pharmacol* **73**:1502–1512.
- Bass SE, Sienkiewicz P, Macdonald CJ, Cheng RY, Sparatore A, Del Soldato P, Roberts DD, Moody TW, Wink DA, and Yeh GC (2009) Novel dithiolethione-modified nonsteroidal anti-inflammatory drugs in human hepatoma HepG2 and colon LS180 cells. *Clin Cancer Res* **15**:1964–1972.
- Bastie CC, Zong H, Xu J, Busa B, Judex S, Kurland IJ, and Pessin JE (2007) Integrative metabolic regulation of peripheral tissue fatty acid oxidation by the SRC kinase family member Fyn. *Cell Metab* **5**:371–381.
- Bieder A, Decouvelaere B, Gaillard C, Depaire H, Heusse D, Ledoux C, Lemar M, Le Roy JP, Raynaud L, Snozzi C, et al. (1983) Comparison of the metabolism of oltipraz in the mouse, rat and monkey and in man. Distribution of the metabolites in each species. *Arzneimittelforschung* **33**:1289–1297.
- Bolton MG, Muñoz A, Jacobson LP, Groopman JD, Maxuitenko YY, Roebuck BD, and Kensler TW (1993) Transient intervention with oltipraz protects against aflatoxin-induced hepatic tumorigenesis. *Cancer Res* **53**:3499–3504.
- Browning JD and Horton JD (2004) Molecular mediators of hepatic steatosis and liver injury. *J Clin Invest* **114**:147–152.

- Büchner N, Altschmied J, Jakob S, Saretzki G, and Haendeler J (2010) Well-known signaling proteins exert new functions in the nucleus and mitochondria. *Antioxid Redox Signal* **13**:551–558.
- Choi SH, Kim YW, and Kim SG (2010) AMPK-mediated GSK3 β inhibition by isoliquiritigenin contributes to protecting mitochondria against iron-catalyzed oxidative stress. *Biochem Pharmacol* **79**:1352–1362.
- Cocco T, Di Paola M, Papa S, and Lorusso M (1999) Arachidonic acid interaction with the mitochondrial electron transport chain promotes reactive oxygen species generation. *Free Radic Biol Med* **27**:51–59.
- Cui QL, Zheng WH, Quirion R, and Almazan G (2005) Inhibition of Src-like kinases reveals Akt-dependent and -independent pathways in insulin-like growth factor I-mediated oligodendrocyte progenitor survival. *J Biol Chem* **280**:8918–8928.
- Das S, Wong R, Rajapakse N, Murphy E, and Steenbergen C (2008) Glycogen synthase kinase 3 inhibition slows mitochondrial adenine nucleotide transport and regulates voltage-dependent anion channel phosphorylation. *Circ Res* **103**:983–991.
- Donlin LT, Roman CA, Adlam M, Regelman AG, and Alexandropoulos K (2002) Defective thymocyte maturation by transgenic expression of a truncated form of the T lymphocyte adapter molecule and Fyn substrate, Sin. *J Immunol* **169**:6900–6909.
- Dwyer JH, Allayee H, Dwyer KM, Fan J, Wu H, Mar R, Luscis AJ, and Mehrabian M (2004) Arachidonate 5-lipoxygenase promoter genotype, dietary arachidonic acid, and atherosclerosis. *N Engl J Med* **350**:29–37.
- George DK, Goldwurm S, MacDonald GA, Cowley LL, Walker NI, Ward PJ, Jazwinska EC, and Powell LW (1998) Increased hepatic iron concentration in nonalcoholic steatohepatitis is associated with increased fibrosis. *Gastroenterology* **114**:311–318.
- Glintborg B, Weimann A, Kensler TW, and Poulsen HE (2006) Oltipraz chemoprevention trial in Qidong, People's Republic of China: unaltered oxidative biomarkers. *Free Radic Biol Med*

41:1010–1014.

Hayashi T, Hirshman MF, Fujii N, Habinowski SA, Witters LA, and Goodyear LJ (2000) Metabolic stress and altered glucose transport: activation of AMP-activated protein kinase as a unifying coupling mechanism. *Diabetes* **49**:527–531.

Hezel AF and Bardeesy N (2008) LKB1; linking cell structure and tumor suppression. *Oncogene* **27**:6908–6919.

Ido Y, Carling D and Ruderman N (2002) Hyperglycemia-induced apoptosis in human umbilical vein endothelial cells: inhibition by the AMP-activated protein kinase activation. *Diabetes* **51**:159–167.

Isenberg JS, Jia Y, Field L, Ridnour LA, Sparatore A, Del Soldato P, Sowers AL, Yeh GC, Moody TW, Wink DA, et al. (2007) Modulation of angiogenesis by dithiolethione-modified NSAIDs and valproic acid. *Br J Pharmacol* **151**:63–72.

Jacobson LP, Zhang BC, Zhu YR, Wang JB, Wu Y, Zhang QN, Yu LY, Qian GS, Kuang SY, Li YF, et al. (1997) Oltipraz chemoprevention trial in Qidong, People's Republic of China: study design and clinical outcomes. *Cancer Epidemiol Biomarkers Prev* **6**:257–265.

Kang KW, Cho IJ, Lee CH, and Kim SG (2003) Essential role of phosphatidylinositol 3-kinase-dependent CCAAT/enhancer binding protein beta activation in the induction of glutathione S-transferase by oltipraz. *J Natl Cancer Inst* **95**:53–66.

Kay HY, Yang JW, Kim TH, Lee DY, Kang B, Ryu JH, Jeon R, and Kim SG (2010) Ajoene, a stable garlic by-product, has an antioxidant effect through Nrf2-mediated glutamate-cysteine ligase induction in HepG2 cells and primary hepatocytes. *J Nutr* **140**:1211–1219.

Kay HY, Kim YW, Ryu DH, Sung SH, Hwang SJ, and Kim SG (2011) Nrf2-mediated liver protection by sauchinone, an antioxidant lignan, from acetaminophen toxicity through the PKC δ -GSK3 β pathway. *Br J Pharmacol* **163**:1653–1665.

Kensler TW and Wakabayashi N (2010) Nrf2: friend or foe for chemoprevention? *Carcinogenesis*

31:90–99.

- Kim SG, Kim YM, Choi YH, Lee MG, Choi JY, Han JY, Cho SH, Jang JW, Um SH, Chon CY, et al. (2010) Pharmacokinetics of oltipraz and its major metabolite (RM) in patients with liver fibrosis or cirrhosis: relationship with suppression of circulating TGF-beta1. *Clin Pharmacol Ther* **88**:360–368.
- Kim YW, Lee SM, Shin SM, Hwang SJ, Brooks JS, Kang HE, Lee MG, Kim SC, and Kim SG (2009) Efficacy of sauchinone as a novel AMPK-activating lignan for preventing iron-induced oxidative stress and liver injury. *Free Radic Biol Med* **47**:1082–1092.
- Kockeritz L, Doble B, Patel S, and Woodgett JR (2006) Glycogen synthase kinase-3-an overview of an over-achieving protein kinase. *Curr Drug Targets* **7**:1377–1388.
- Kumar S and Bandyopadhyay U (2005) Free heme toxicity and its detoxification systems in human. *Toxicol Lett* **157**:175–188.
- Liu XM, Peyton KJ, Shebib AR, Wang H, Korhuis RJ, and Durante W (2011) Activation of AMPK stimulates heme oxygenase-1 gene expression and human endothelial cell survival. *Am J Physiol Heart Circ Physiol* **300**:H84–H93.
- Lu KV, Zhu S, Cvrljevic A, Huang TT, Sarkaria S, Ahkavan D, Dang J, Dinca EB, Plaisier SB, Oderberg I, et al. (2009) Fyn and SRC are effectors of oncogenic epidermal growth factor receptor signaling in glioblastoma patients. *Cancer Res* **69**:6889–6898.
- McLaren CE, Gordeuk VR, Looker AC, Hasselblad V, Edwards CQ, Griffen LM, Kushner JP, and Brittenham GM (1995) Prevalence of heterozygotes for hemochromatosis in the white population of the United States. *Blood* **86**:2021–2027.
- Mustelin T, Pessa-Morikawa T, Autero M, Gassmann M, Andersson LC, Gahmberg CG, and Burn P (1992) Regulation of the p59fyn protein tyrosine kinase by the CD45 phosphotyrosine phosphatase. *Eur J Immunol* **22**:1173–1178.
- Nguyen T, Yang CS, and Pickett CB (2004) The pathways and molecular mechanisms regulating Nrf2 activation in response to chemical stress. *Free Radic Biol Med* **37**:433–441.

- Nishihara M, Miura T, Miki T, Tanno M, Yano T, Naitoh K, Ohori K, Hotta H, Terashima Y, and Shimamoto K (2007) Modulation of the mitochondrial permeability transition pore complex in GSK-3 β -mediated myocardial protection. *J Mol Cell Cardiol* **43**:564–570.
- O'Dwyer PJ, Clayton M, Halbherr T, Myers CB, and Yao K (1997) Cellular kinetics of induction by oltipraz and its keto derivative of detoxication enzymes in human colon adenocarcinoma cells. *Clin Cancer Res* **3**:783–791.
- O'Dwyer PJ, Szarka C, Brennan JM, Laub PB, and Gallo JM (2000) Pharmacokinetics of the chemopreventive agent oltipraz and of its metabolite M3 in human subjects after a single oral dose. *Clin Cancer Res* **6**:4692–4696.
- Pariser H, Ezquerra L, Herradon G, Perez-Pinera P, and Deuel TF (2005) Fyn is a downstream target of the pleiotrophin/receptor protein tyrosine phosphatase beta/zeta-signaling pathway: regulation of tyrosine phosphorylation of Fyn by pleiotrophin. *Biochem Biophys Res Commun* **332**:664–669.
- Parsons SJ and Parsons JT (2004) Src family kinases, key regulators of signal transduction. *Oncogene* **23**:7906–7909.
- Peters DJ, McGrew BR, Perron DC, Liptak LM, and Laudano AP (1990) In vivo phosphorylation and membrane association of the fyn proto-oncogene product in IM-9 human lymphoblasts. *Oncogene* **5**:1313–1319.
- Ricci JE, Lang V, Luciano F, Belhacene N, Giordanengo V, Michel F, Bismuth G, and Auberger P (2001) An absolute requirement for Fyn in T cell receptor-induced caspase activation and apoptosis. *FASEB J* **15**:1777-1779.
- Salazar M, Rojo AI, Velasco D, de Sagarra RM, and Cuadrado A (2006) Glycogen synthase kinase-3 β inhibits the xenobiotic and antioxidant cell response by direct phosphorylation and nuclear exclusion of the transcription factor Nrf2. *J Biol Chem* **281**:14841–14851.
- Sandilands E, Brunton VG, Frame MC (2007) The membrane targeting and spatial activation of Src, Yes and Fyn is influenced by palmitoylation and distinct RhoB/RhoD endosome requirements. *J Cell Sci* **120**:2555–2564.

- Scorrano L, Penzo D, Petronilli V, Pagano F, and Bernardi P (2001) Arachidonic acid causes cell death through the mitochondrial permeability transition. Implications for tumor necrosis factor- α apoptotic signaling. *J Biol Chem* **276**:12035–12040.
- Shin SM, Cho IJ, and Kim SG (2009) Resveratrol protects mitochondria against oxidative stress through AMP-activated protein kinase-mediated glycogen synthase kinase-3 β inhibition downstream of poly(ADP-ribose)polymerase-LKB1 pathway. *Mol Pharmacol* **76**:884–895.
- Shin SM and Kim SG (2009) Inhibition of arachidonic acid and iron-induced mitochondrial dysfunction and apoptosis by oltipraz and novel 1,2-dithiole-3-thione congeners. *Mol Pharmacol* **75**:242–253.
- Simopoulos AP (2006) Evolutionary aspects of diet, the omega-6/omega-3 ratio and genetic variation: nutritional implications for chronic diseases. *Biomed Pharmacother* **60**:502–507.
- Tazzari V, Cappelletti G, Casagrande M, Perrino E, Renzi L, Del Soldato P, and Sparatore A (2010) New aryldithiolethione derivatives as potent histone deacetylase inhibitors. *Bioorg Med Chem* **18**:4187–4194.
- Terai K, Hiramoto Y, Masaki M, Sugiyama S, Kuroda T, Hori M, Kawase I and Hirota H (2005) AMP-activated protein kinase protects cardiomyocytes against hypoxic injury through attenuation of endoplasmic reticulum stress. *Mol Cell Biol* **25**:9554–9575.
- Thompson TN (2001) Optimization of metabolic stability as a goal of modern drug design. *Med Res Rev* **21**:412–449.
- Wang JS, Shen X, He X, Zhu YR, Zhang BC, Wang JB, Qian GS, Kuang SY, Zarba A, Egner PA, et al. (1999) Protective alterations in phase 1 and 2 metabolism of aflatoxin B1 by oltipraz in residents of Qidong, People's Republic of China. *J Natl Cancer Inst* **91**:347–354.
- Yamada E, Pessin JE, Kurland IJ, Schwartz GJ, and Bastie CC (2010) Fyn-dependent regulation of energy expenditure and body weight is mediated by tyrosine phosphorylation of LKB1. *Cell Metab* **11**:113–124.

Zamzami N and Kroemer G (2001) The mitochondrion in apoptosis: how Pandora's box opens. *Nat Rev Mol Cell Biol* **2**:67–71.

Zhang Y and Munday R (2008) Dithiolethiones for cancer chemoprevention: where do we stand? *Mol Cancer Ther* **7**:3470–3479.

FOONOTES

This work was supported by the National Research Foundation of Korea grant funded by the Ministry of Education, Science and Technology [2011-0009582] and in part by the World Class University project [R32-2011-000-10098-0].

FIGURE LEGENDS

Fig. 1. The effects of dithiolethiones on the viability of HepG2 cells

A) The chemical structures of dithiolethione derivatives. B) The ED₅₀ values of dithiolethiones for cell viability. HepG2 cells were treated with 0.3-30 μM dithiolethione congeners for 1 h, and continuously incubated with 10 μM arachidonic acid (AA) for the next 12 h. After washing, the cells were challenged with 5 μM iron for 6 h with or without each agent. Cell survival was measured using MTT assays. Data represent the mean ± S.E.M. of six replicates.

Fig. 2. Inhibition of apoptotic injury by dithiolethiones

A) MTT assays. HepG2 cells were treated with 0.3-30 μM of each dithiolethione congener (upper) for 1 h and continuously incubated with 10 μM AA for the next 12 h. After washing, the cells were challenged with 5 μM iron for 6 h with the agent of interest. Cells were also incubated with each agent alone for 19 h (inset). Cell viability was measured using MTT assays. Data represent the mean ± S.E.M. of six replicates. B) Representative photographs of cell morphology. Light microscopy shows the morphology of cells treated as described above (200x). Images have been inverted for visual clarity. C) Immunoblottings for the proteins associated with apoptosis. Proteins were immunoblotted on the cell lysates.

Fig. 3. Prevention of mitochondrial injury by dithiolethiones

A) Mitochondrial membrane permeability (MMP). HepG2 cells were challenged with 30 μM of each agent for 1 h, followed by incubation with AA (12 h) and iron (6 h). They were collected after Rhodamine 123 (Rh123) staining. M1 fraction indicates cells with low intensity of Rh123 fluorescence. The percentage of M1 population was quantified. Data represent the mean ± S.E.M. of three separate experiments. The statistical significance of differences between treatments and either the vehicle-treated control (**p<0.01) or cells treated with AA + iron ([#]p<0.01) was determined (N.S., not significant). B) Superoxide production in the mitochondria. Cells were exposed to 30 μM of each

dithiolethione congener for 1 h and subsequently to 10 μ M AA (12 h), followed by incubation with 5 μ M iron for 6 h, and were stained with MitoSOX. Increase in fluorescence indicates mitochondrial superoxide production. Results were confirmed by repeated experiments. C) Analyses of cell-cycle progression using flow cytometry. Cells were treated as described above.

Fig. 4. The role of AMPK activation by CDTs in mitochondrial membrane permeability.

A) AMPK activation. Immunoblot analyses were performed on the lysates of cells treated with 30 μ M of each agent for 1 h. Oltipraz (30 μ M) was used as a positive control. B) Inhibitory phosphorylation of GSK3 β . C) Reduced mitochondrial protective effect by DN-AMPK. After infection with adenoviral DN-AMPK for 12 h, HepG2 cells were treated with SNU1A (10 μ M) for 1 h and continuously exposed to AA + iron. Rh123-negative cell population was measured in the cells. For A and C, data represent the mean \pm S.E.M. with four separate experiments (significant compared to respective vehicle-treated control, ** p <0.01; N.S., not significant). D) Immunoblottings for pACC or pGSK3 β . Immunoblottings were done on the lysates of HepG2 cells treated with SNU1A for 12 h after infection of Ad-LacZ or Ad-DN-AMPK.

Fig. 5. Fyn inhibition by dithiolethiones for mitochondrial protection

A) The inhibition of Fyn phosphorylation. Fyn immunoprecipitates were immunoblotted with anti-phospho-tyrosine antibody. SU6656, a Fyn inhibitor, was used as a positive control. Cells were treated with 30 μ M dithiolethione congener or 10 μ M SU6656 and subsequently exposed to 10 μ M AA (12h), followed by incubation with 5 μ M iron for 30 min. B) Inhibition of basal Fyn phosphorylation. Cells were treated with 30 μ M SNU1A or 10 μ M SU6656 for 1 h. C) *In vitro* kinase assays. Experimental details were described in Material and Methods section. The data represent the means of duplicate determinations. D) Reversal by Fyn overexpression of decrease in Rh123-negative cell population. After Fyn overexpression, HepG2 cells were incubated with SNU1A (10 μ M) for 1 h and continuously exposed to AA (12 h) + iron (6 h). Rh123-negative cell population was analyzed as

described in the legend to Fig. 3A. Data represent the mean \pm S.E.M. of three separate experiments. E) Reversal by Fyn overexpression of SNU1A effect on AMPK activation. After Fyn transfection, cells were treated with 10 μ M SNU1A for 1 h. O/E, overexpression. For A, B, and D, the statistical significance of differences between treatments and either the vehicle-treated control (* p <0.05, ** p <0.01), or cells treated with AA + iron ([#] p <0.05, ^{##} p <0.01; N.S., not significant).

Fig. 6. Enhancement of antioxidant capacity by dithiolethiones

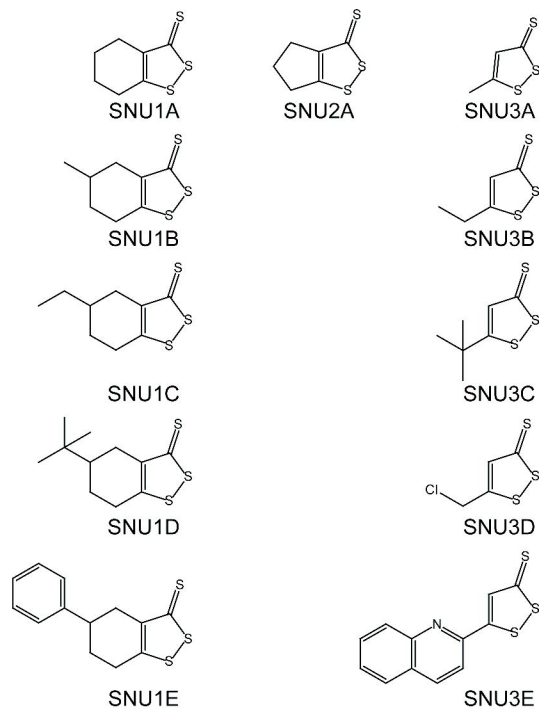
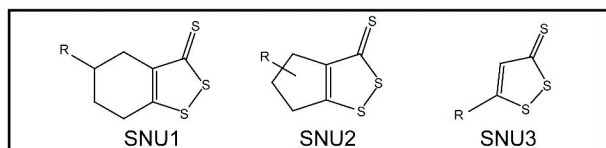
A) The cellular GSH contents. The GSH content was assessed in HepG2 cells treated as described in the legend to Fig. 2A (left). Cells were also treated with 30 μ M of each agent alone for 18 h (right). B) DCF fluorescence assays. H₂O₂ production was monitored using DCF fluorescence. HepG2 cells were treated with 30 μ M of each agent for 1 h, and were incubated with AA (12 h) and iron (6 h). Results were confirmed by three separate experiments. C) The effect of Fyn overexpression and Compound C treatment on the increase in GSH content. Cells were transfected with Mock vector or Fyn, and continuously exposed to SNU1A (10 μ M, 18 h) with or without Compound C pre-treatment (10 μ M, 1 h). O/E, overexpression. For A and C, data represent the mean \pm S.E.M. of three separate experiments. The statistical significance of differences between treatments and either the vehicle-treated control (* p <0.05, ** p <0.01) or cells treated with AA + iron ([#] p <0.05, ^{##} p <0.01; N.S., not significant) was determined.

Fig. 7. Nrf2 –ARE activation by dithiolethiones

A) DCF fluorescence assays. HepG2 cells were treated with 30 μ M each agent alone for 6 h. Results were confirmed by three separate experiments. B) Immunoblottings for Nrf2. Nrf2 was immunoblotted on the lysates of cells treated with each agent for 12 h. The relative band intensity of Nrf2 to β -actin was assessed by scanning densitometry of the immunoblots. C) NQO1-ARE reporter gene assays. The luciferase reporter activity was measured in cells treated with SNU compounds for 12 h. D) The effects of Ad-DN-AMPK on Nrf2 and ARE reporter activity. HepG2 cells were treated

as described in the legend to Fig. 4D (upper). After adenoviral DN-AMPK infection, cells were treated with SNU1A for 12 h (lower). E) The effects of Fyn overexpression on Nrf2 and ARE reporter activity. Cells were treated as described above. For C, D, and E, values represent mean \pm S.E.M. from 5 independent experiments (treatment mean significantly different from vehicle-treated control, (*p<0.05, **p<0.01, N.S., not significant).

Fig. 8. A schematic diagram illustrating the proposed mechanism by which cycloalkane-fused dithiolethiones protect cells from oxidative injury



Compounds	R	ED ₅₀ (μM)
SNU1A	H	2.98±0.77
SNU1B	Methyl	3.86±1.46
SNU1C	Ethyl	1.72±1.18
SNU1D	<i>t</i> -Butyl	3.78±1.50
SNU1E	Phenyl	3.00±1.27
SNU2A	H	3.20±0.77
SNU3A	Methyl	10.99±1.80
SNU3B	Ethyl	6.71±1.22
SNU3C	<i>t</i> -Butyl	9.87±1.52
SNU3D	Chloromethyl	>50
SNU3E	2-Quinolyl	>50

Fig. 1

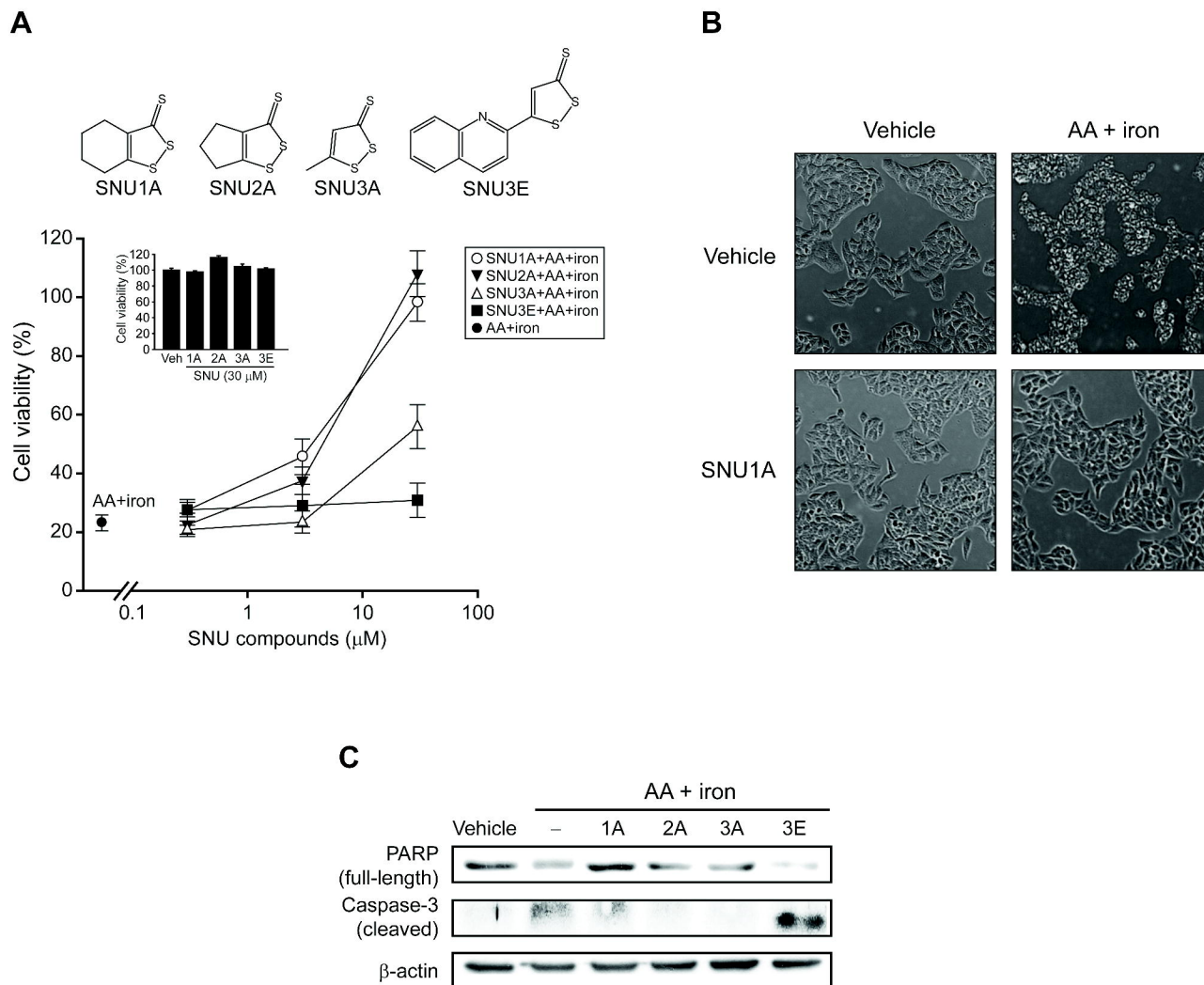
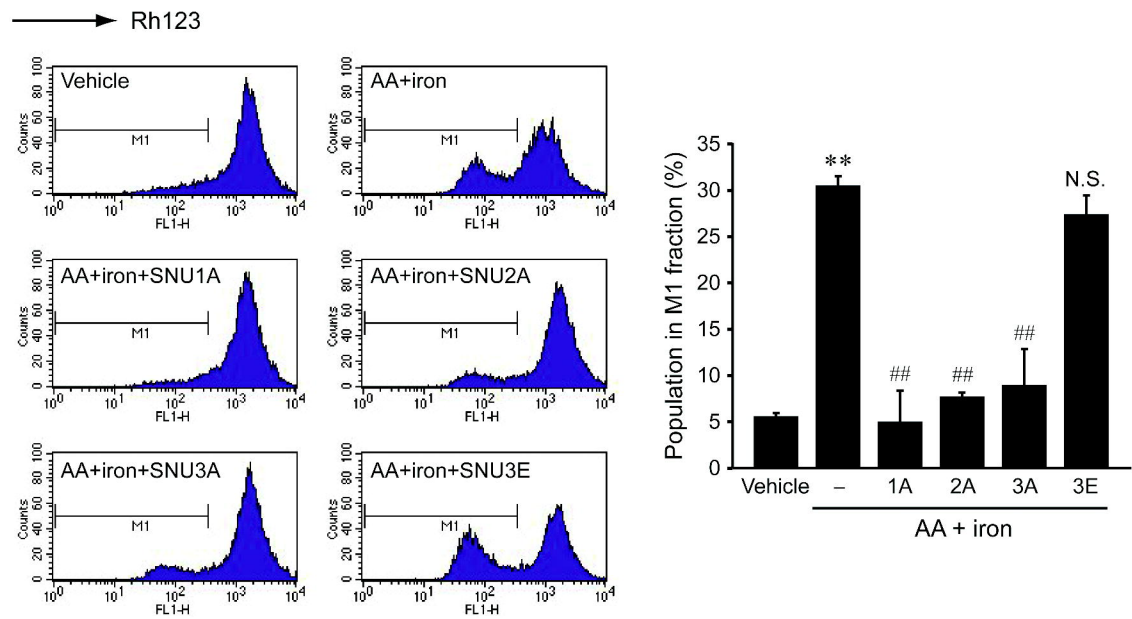
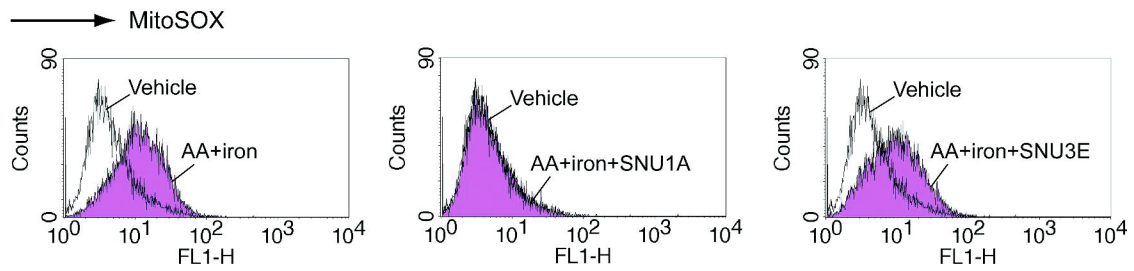


Fig. 2

A



B



C

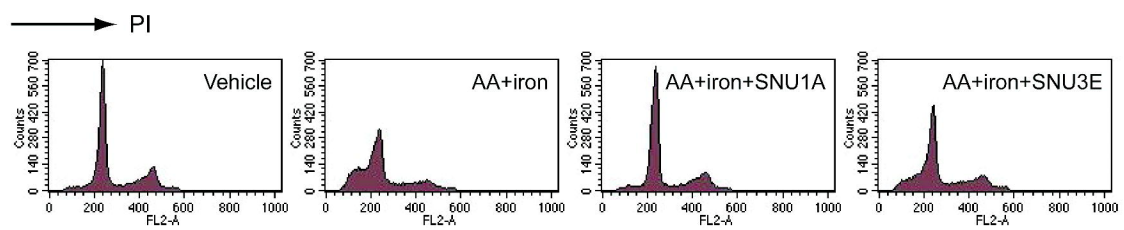


Fig. 3

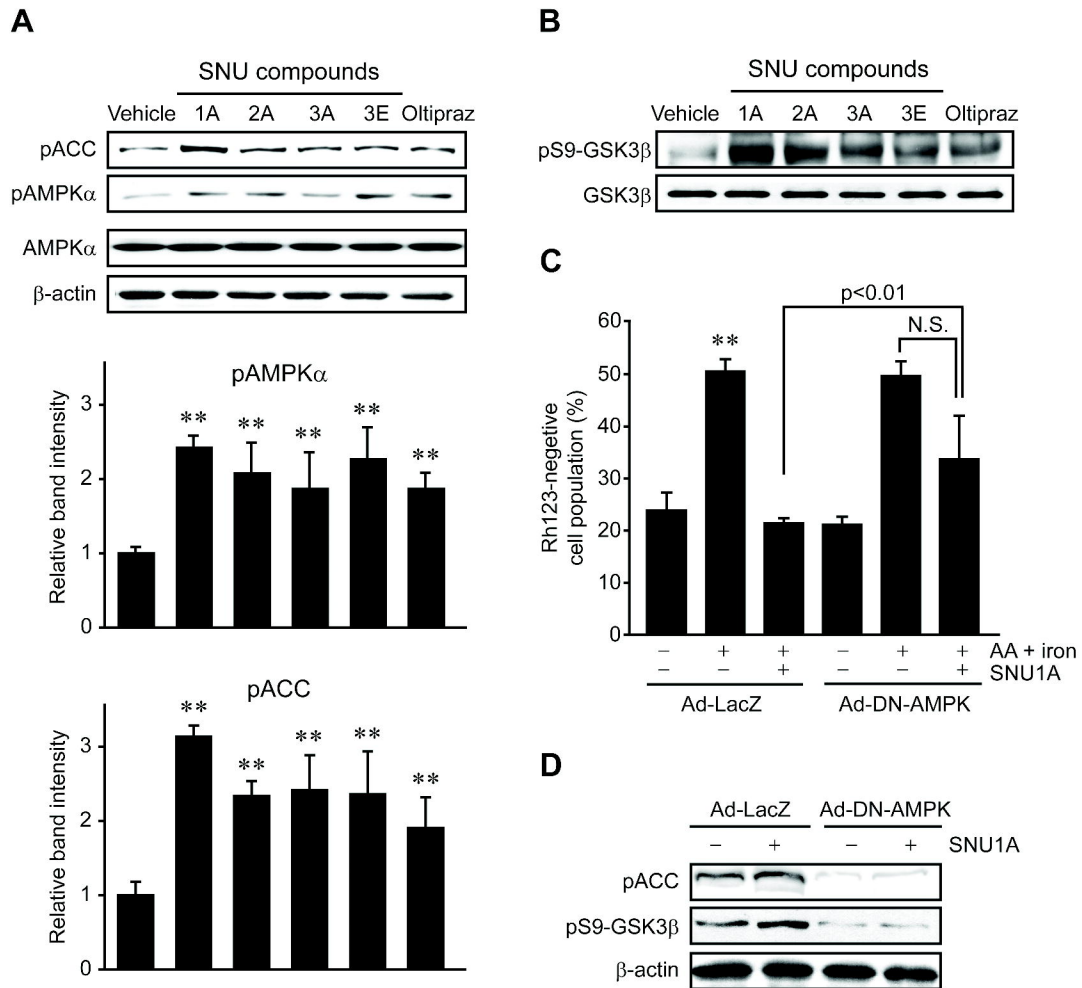


Fig. 4

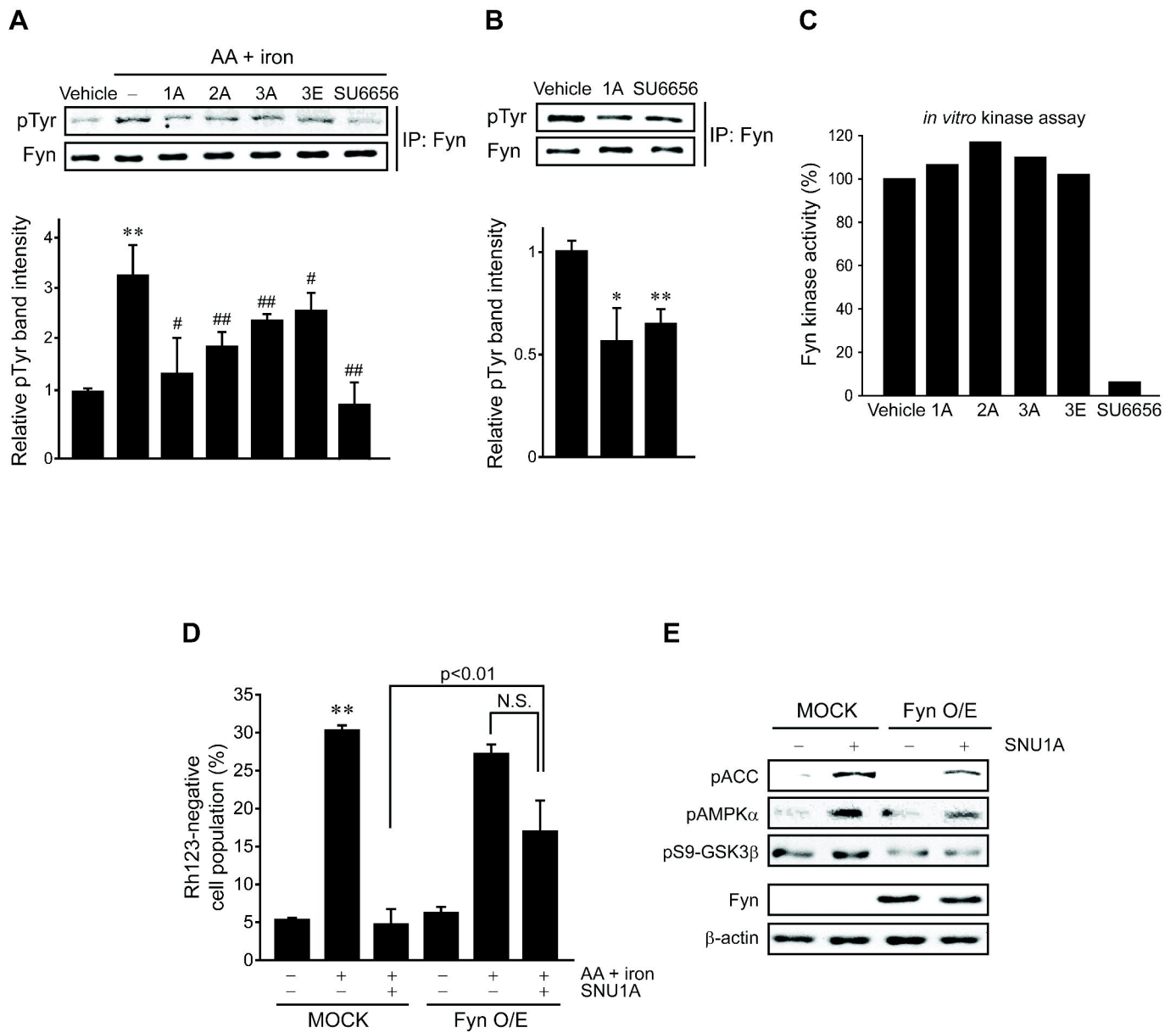


Fig. 5

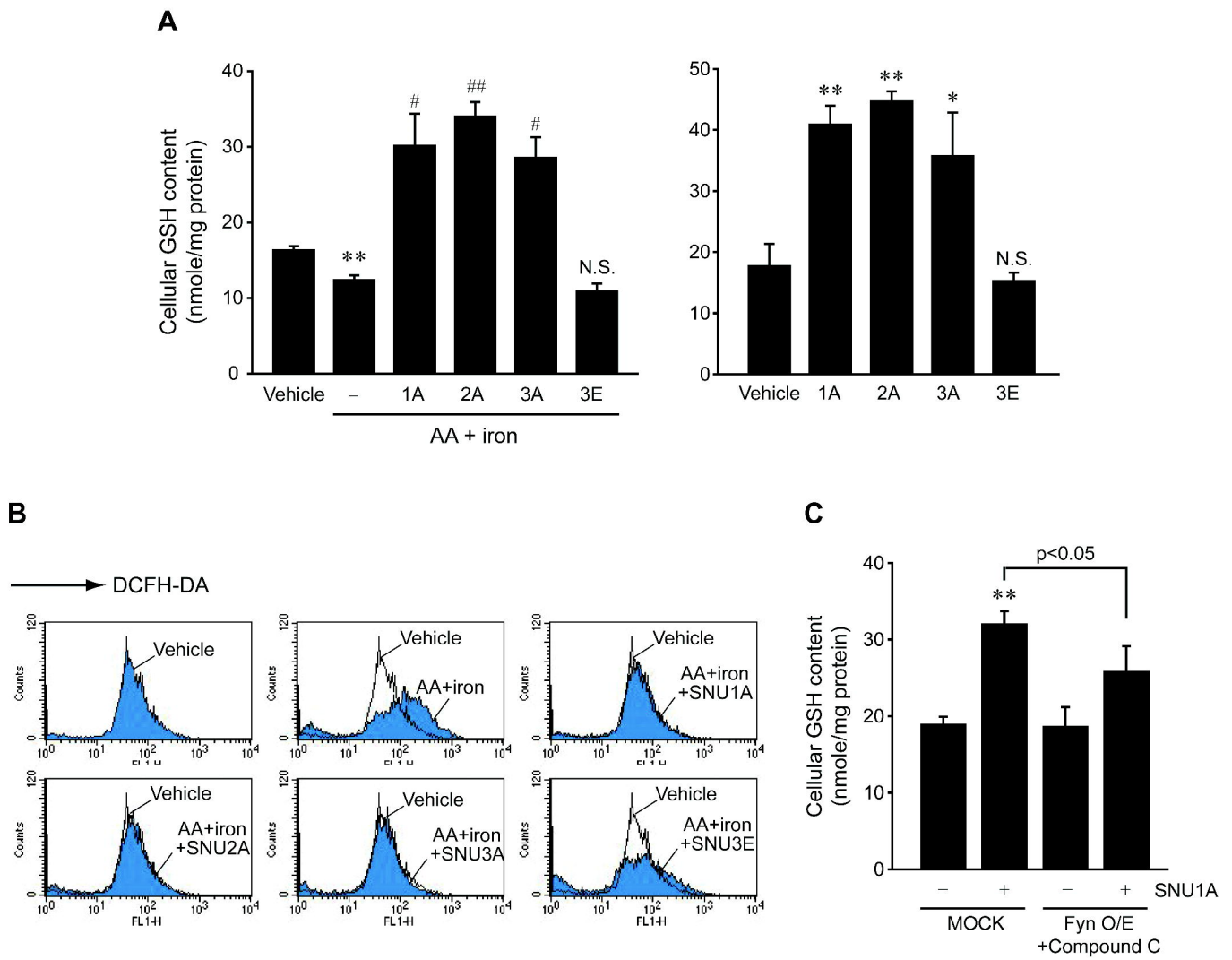
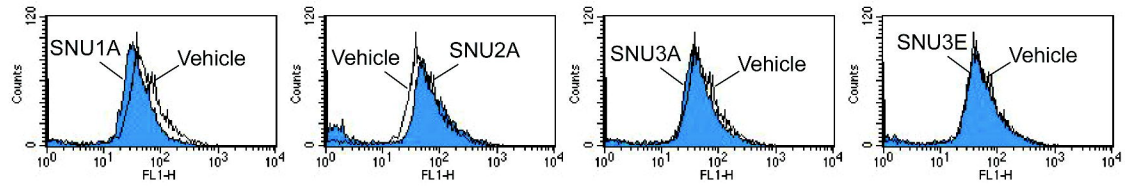
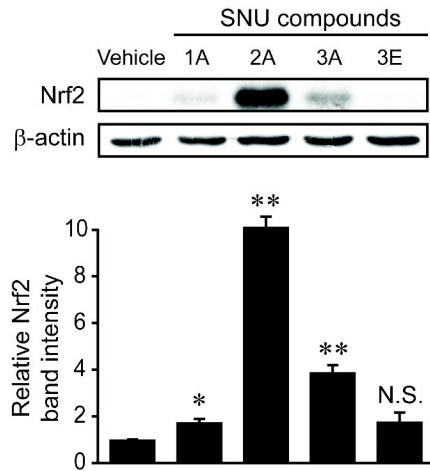
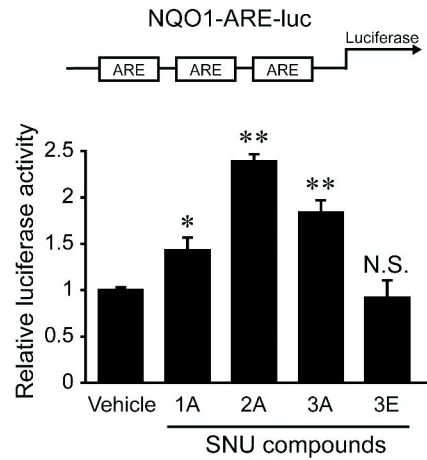
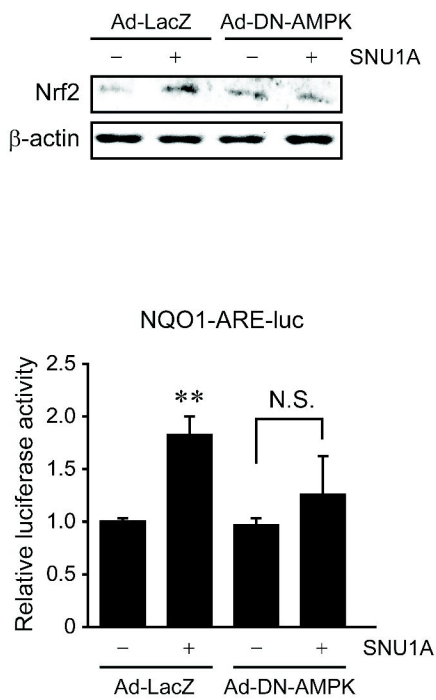
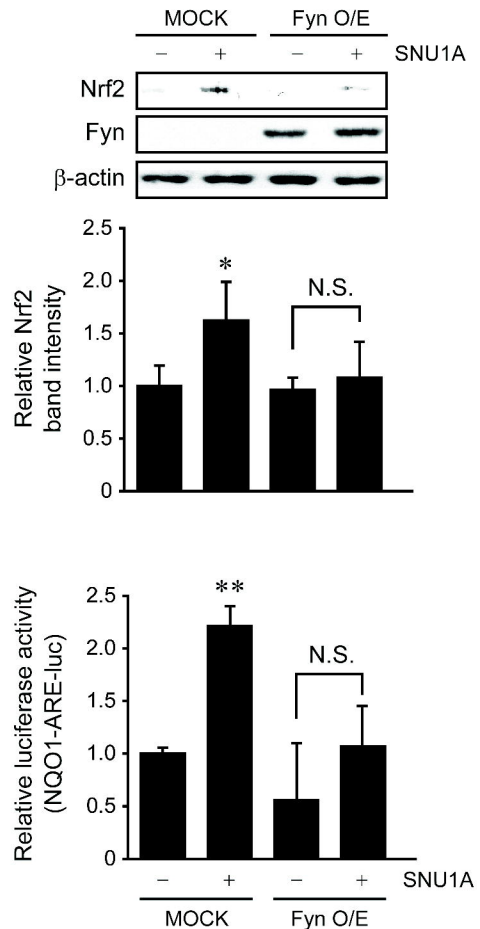


Fig. 6

A

Molecular Pharmacology Fast Forward. Published on April 2, 2012 as DOI: 10.1124/mol.111.077149
 → **TDCFHDA** has not been copyedited and formatted. The final version may differ from this version.

**B****C****D****E****Fig. 7**

